J. Fluid Mech. (1982), *vol.* 120, *pp.* 385–409
Printed in Great Britain

LDV measurements of an air–solid two-phase flow in a horizontal pipe

By YUTAKA TSUJI AND YOSHINOBU MORIKAWA
Faculty of Engineering, Osaka University, Osaka, Japan

(Received 7 July 1981)

Measurements of air and solid velocities were made in an air–solid two-phase flow in a horizontal pipe by the use of a laser-Doppler velocimeter (LDV). The pipe was 30 mm inner diameter, and two kinds of plastic particles, 0·2 and 3·4 mm in diameter, were conveyed in addition to fine particles (ammonium chloride) for air-flow detection. The air velocities averaged over the pipe cross section ranged from 6 to 20 m/s and the solid-to-air mass-flow ratio was up to 6. Simultaneous measurements of both air and 0·2 mm particle velocities were found possible by setting threshold values against the pedestal and Doppler components of the photomultiplier signal.

As the loading ratio increased and the air velocity decreased, mean-velocity distributions of both phases increased asymmetrical tendency. In the presence of 0·2 mm particles, a flattening of the velocity profile was remarkable. The effects of the solid particles on air-flow turbulence varied greatly with particle size. That is, 3·4 mm particles increased the turbulence markedly, while 0·2 mm ones reduced it. The probability-density function of the air flow deviated from the normal distribution (Gaussian) in the presence of particles. Finally, the frequency spectra of air-flow turbulence were obtained in the presence of 0·2 mm particles by using a fast Fourier transform (FFT). As a result, it was found that the higher-frequency components increased with increasing loading ratio.

1. Introduction

Laser-Doppler velocimetry (LDV) is becoming popular for fluid measurements, although it is still rather expensive. As is well known, the most outstanding merit of the LDV is that it does not intrude into the flow. LDV makes it possible to measure fluid velocities that cannot be measured by conventional Pitot tubes and hot-wire anemometers. Hence the usefulness of LDV is clearly acknowledged at present. However, when we try to apply LDV technique to some flows, we must cope with several difficulties that are inherent to the flows. Since basic aspects of the LDV technique have been established, various examples of LDV measurements are now being accumulated by many workers. The present paper deals with such an application of LDV to two-phase flow. This paper shows the results that the authors obtained in an air–solid two-phase flow in a horizontal pipe. Below we describe previous work on the air–solid two-phase flow in a pipe.

The air–solid two-phase flow in a pipe has long been investigated in connection with pneumatic conveying of solid particles. Pneumatic-conveying facilities consist of a blower, solid feeder, transportation pipe and receiver of the solids. Phenomena in

the transportation pipe are the most interesting from the fluid-dynamic viewpoint. It was in the 1920s and 1930s that research about the flow in such a pipe started, which investigated the relation between the particle flow rate and pressure drop. Gasterstädt (1924), a pioneer in those days, took instantaneous photographs of flying particles. Subsequently, research with the same pattern has been done, theoretically and experimentally. Namely, researchers have been making measurements of the pressure drop due to the presence of particles, and have been seeking equations correlating experimental data by the use of various empirical coefficients. Since the pressure drop is the most important quantity in estimating the power required for transportation, it is natural that the pressure drop was studied first of all. Even now, the importance of the pressure drop is not altered. However, the problem is that available methods for predicting the pressure drop are not satisfactory, even though a number of experiments have been carried out for various sorts of particles and given conditions. Eventually, we must realize that, no matter how many measurements of one-dimensional quantities like the pressure drop are made, we cannot make progress in treating this flow unless we obtain information about its internal structure. A few research workers tried to obtain behaviour of the particles by using high-speed ciné cameras (Adam 1957; Doig & Roper 1967; Jotaki & Tomita 1971) and other optical methods (Kramer & Depew 1972). However, they did not get detailed information about the gaseous phase. That is because hot-wire probes cannot be used, owing to solid particles moving at high velocities. For the moment, the object of the study of the air–solid two-phase flow is to clarify the flow mechanism resulting from interaction between gaseous and solid phases. To achieve this, new devices have been required. The LDV is considered to be such a device, by which further progress in the research is expected.

LDV requires the presence of seeded particles as light scatterers. In that sense the LDV technique has been considered to be suited to two-phase flow, which includes particles naturally. In fact most previous works using LDV in two-phase flow were concerned with the measurements of the velocity, concentration and size of such particles (e.g. Durst & Umhauer 1975; Birchenough & Mason 1976). In contrast, there have been very few works dealing with the gaseous phase, even if LDV has been used. This situation is the motivation of the present work. In order to detect the fluid motion, we must seed small scattering particles, in addition to the large particles that are conveyed in the pipe. In this work, a frequency tracker was used to process the signal from a photomultiplier. Simultaneous measurements of air and solid velocities were attempted by developing a special signal-processing device.

2. Experimental equipment and method

2.1. *Pipeline*

Figure 1 shows the experimental pipeline. The air was supplied by a turbo-blower and passed the flow-rate measuring section where a Pitot tube was set up. A part of the air passed the small particle-generating chamber, which provided scattering particles, and returned to the main pipe. The air was mixed with large particles at the particle-feeding point and driven to the horizontal test section as a two-phase flow. The internal diameter of the test pipe was 30·5 mm, and the test section was made of a glass pipe whose wall thickness was 0·75 mm. The distance between the mixing point

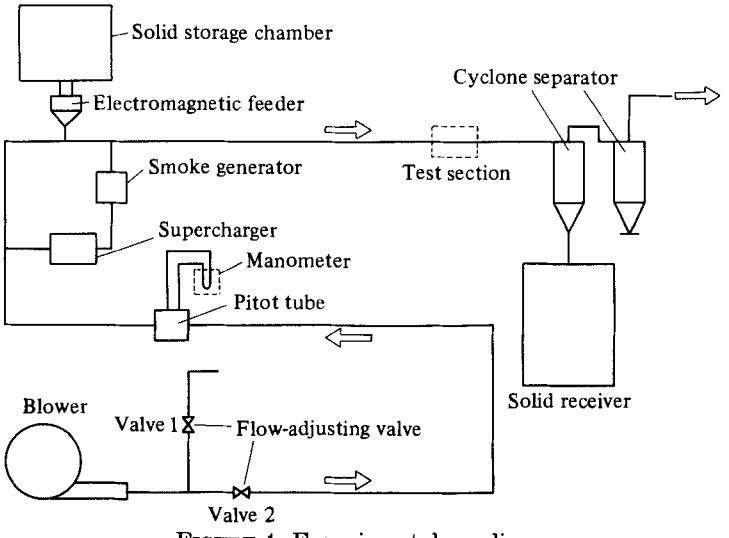

FIGURE 1. Experimental pipeline.

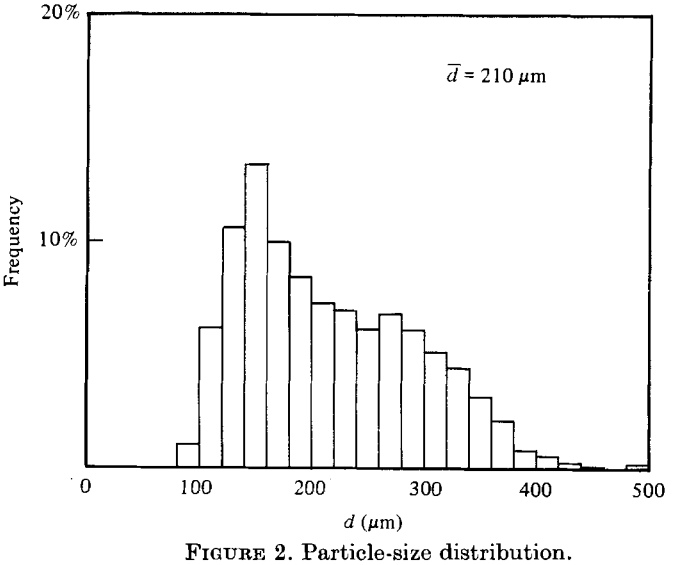

FIGURE 2. Particle-size distribution.

and the test section was 3560 mm. Two kinds of plastic pellets were used, with mean diameters of 3·4 mm and 0·2 mm and density 1000 kg/m^3. These particles were supplied by an electromagnetic feeder and separated from air by a cyclone separator. The larger particles of the above two kinds were regarded as monodisperse particles, but the smaller ones had a rather wide size distribution shown in figure 2. Fine tracers seeded for detecting the air flow were ammonium chloride smoke particles of mean diameter 0·6 μm. Durst, Melling & Whitelaw (1976) mentioned that particles produced by such chemical reaction are not suitable for LDV because of poor controllability of the concentration rate. We solved this problem by developing a specially designed generator. Figure 3 shows the size distribution of the ammonium chloride particles captured at the test section. The concentration of the smoke was adjusted high

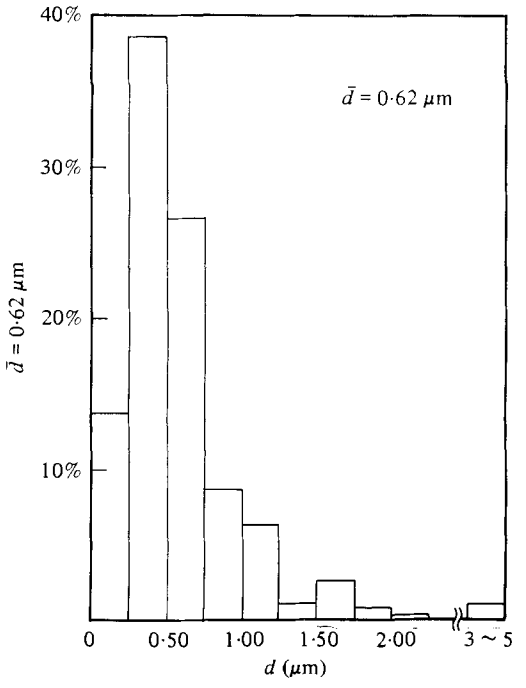

FIGURE 3. Size distribution of ammonium chloride particles.

enough that the spectrum of the tracker output compared well with that of a hot-wire anemometer up to several kHz in a single phase flow. We had to clean the test pipe out after about 20 minutes of measurement, because the fine particles tended to cling to the pipe wall.

2.2. *Optical arrangement and signal-processing system*

Figure 4 shows the optical arrangement and signal-processing system. The fringe-mode system was adopted in this experiment. The beam from a helium–neon laser (15 mW at a wavelength = 6328 Å) was split into two beams 50 mm apart. The two beams were focused by a lens of focal length 100 mm to intersect in the scattering volume within the pipe. Forward-scattered light was collected through lenses of focal length 100 mm on to a photomultiplier. The principal characteristics of the optical system were:

intersection angle between beams	25°,
fringe spacing	1·2 μm,
diameter of scattering volume at e^{-2} intensity	76·2 μm,
length of scattering volume at e^{-2} intensity	250 μm,
number of fringes in scattering volume	41,
frequency-to-velocity conversion factor	0·6838 m s^{-1} MHz^{-1}.

Large particles of several millimetres diameter cause drop-out of the Doppler signal in the case of the forward-scattered-light system. When the particle diameter is reduced from the order of a millimetre to a hundred micrometres, the Doppler signal is

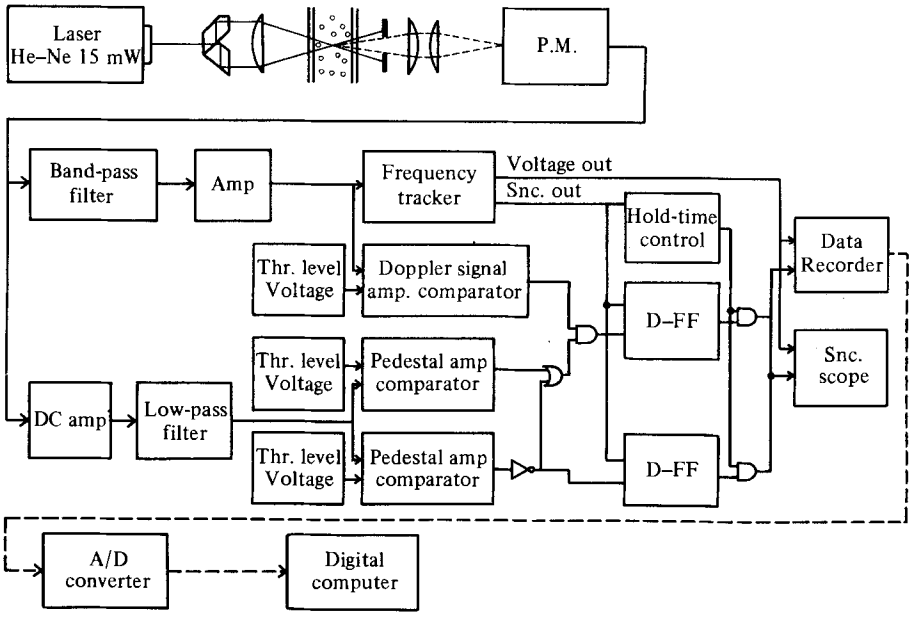

FIGURE 4. Optical arrangement and signal-processing system.

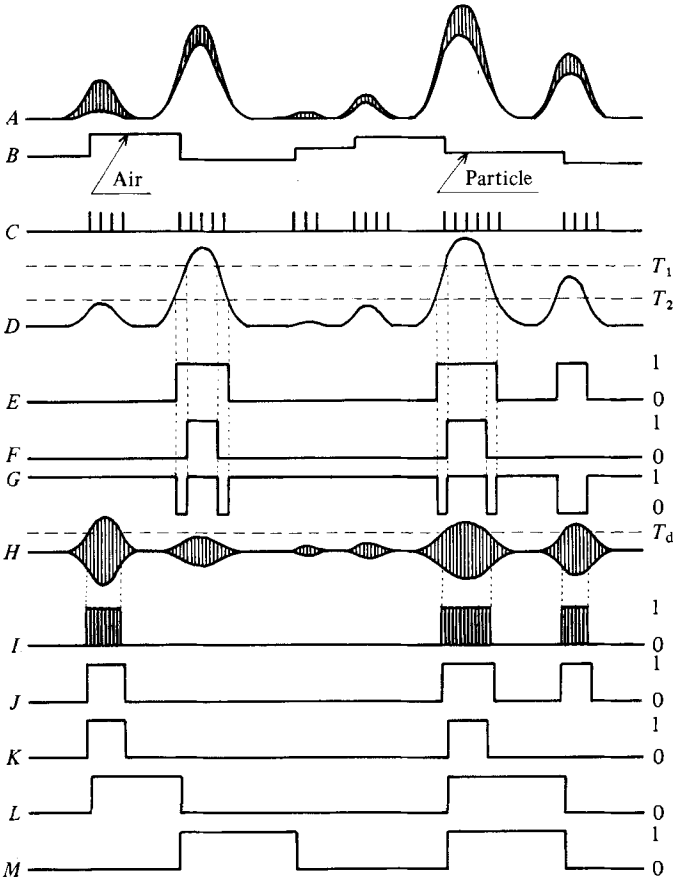

FIGURE 5. Time chart of signals.

obtained from such large particles as well as much smaller tracers of several micrometres. The intensity of the light scattered from the large particles is stronger than that from the small tracers. That is, the light from the large particles has a large pedestal amplitude. Making use of this difference in properties of the scattered light, simultaneous measurements of velocities of both air and solid phases are possible, so long as we succeed in differentiating the signals from both phases into the signals from each of them. However, the pedestal amplitude also depends on which part of the scattering volume with finite dimensions the particles pass through. Therefore a signal separation based on only the pedestal amplitude is insufficient to distinguish between large and small particles. If a comparison of the pedestal amplitude is made for the particles crossing the central part of the scattering volume, the signals of both particles can be distinguished accurately. Doppler signals from those particles have many waveforms. Hence, Maeda, Hishida & Furutani (1980) separated the signals by taking the wavenumber into account in addition to the pedestal amplitude, and measured an air–solid two-phase flow in a vertical pipe. We made an attempt at using the amplitude of the Doppler component. It is known that the Doppler amplitude is large when the particles cross the centre part of the scattering volume. Therefore, effective signals from those particles are obtained by setting a threshold value for the Doppler amplitude. As for the pedestal, we set two threshold values to extract the signals with sufficiently large pedestal and sufficiently small one. The signals with intermediate pedestal amplitude were regarded as ambiguous data and excluded from the subsequent processing. The details of the procedure are described below.

Figure 5 shows a time chart of the signal processing. Signal A is the output from the photomultiplier, where the Doppler component is superimposed on the pedestal one. The signal A is processed with a frequency tracker (KANOMAX model 27-1090), which gives an analogue voltage output B proportional to the Doppler frequency. Signal C is a synchronized pulse which the tracker gives at every moment when it processes the signal A. The procedure to distinguish which parts of signal B correspond to large or small particles is as follows. Signal D, the pedestal component, is obtained by a low-pass filter. Two thresholds T_1 and T_2 are imposed on signal D, and square waves E and F are obtained which correspond to the pedestal amplitude larger than T_1 and smaller than T_2, respectively. Further, signal G is derived from E and F through an exclusive NOR gate. $G = 0$ means that the pedestal amplitude is between T_1 and T_2. In this method, such a signal is regarded as an ambiguous one for which we cannot decide whether it represents a large or small particle. Thus discrimination between effective and ineffective signals with respect to the pedestal is made by referring to the signal G. Along with the above process for the pedestal component, the Doppler component is obtained from signal A by using a high-pass filter. A threshold value T_d is imposed on this Doppler amplitude, and the wave I is obtained by a comparator. By taking the envelope of the wave I, a square wave J is produced that corresponds to the Doppler amplitude larger than T_d. Next, the wave K is obtained from a logical product of G and J by an AND gate. The value of $K = 1$ means that the signal can be distinguished, that is the signal satisfies both conditions (i) that it is not ambiguous with respect to the pedestal amplitude, and (ii) that the Doppler amplitude is sufficiently large. As is noticed in the outputs B and C, the tracker holds the output voltage B when the Doppler signal to be processed disappears. Therefore the time periods of B and K are not necessarily coincident. To make a comparison between B and K

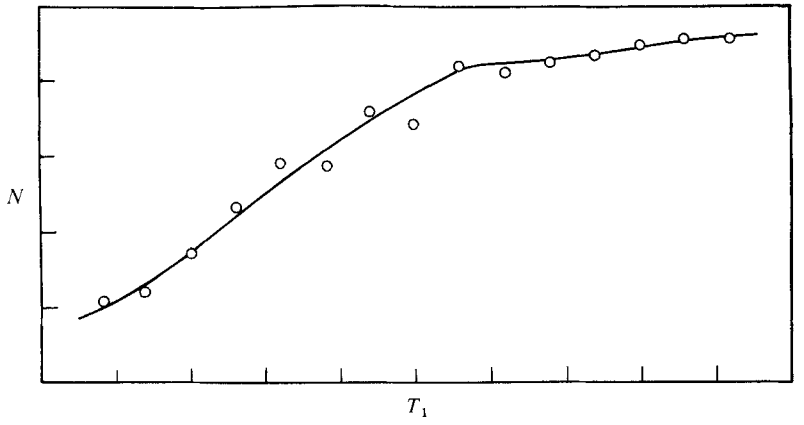

FIGURE 6. Relation between the threshold value T_1 and sample number N.

easy, a D-flip-flop circuit is useful. When K and C are put into the D-FF circuit, signal L is obtained. The value of $L = 1$ corresponds to a distinguishable hold signal. In signal M obtained from F and C through the D-FF circuit, the value of $M = 1$ corresponds to a hold signal which has the large pedestal amplitude. Here discrimination between large and small particles can be made easily in signal B, where the discriminated parts are shown by arrows. That is, the signals of $L = 1$ and $M = 1$ come from the large particles, and those of $L = 1$ and $M = 0$ from the small particles. In the above process, the case of $L = 0$ is rejected as an ambiguous signal. However, usually the large pedestal does not occur from the small particles. Thus it does not make a large difference to accept the signal of $L = 0$ and $M = 1$ as the large particle.

We investigated the effects of the thresholds T_1, T_2 and T_d. For instance, signals having the pedestal amplitude smaller than T_1 were sampled during a certain period. Figure 6 shows the relation between T_1 and the number of samples. The sample number increases as T_1 increases, but the rate of increase is different according to the range of T_1. Namely, the number increases sharply with T_1 at first, but beyond a certain value of T_1 it increases at a smaller rate. This means that samples include almost all signals coming from both large and small particles when T_1 is adjusted to be larger than a critical value. There were also the same critical values in T_2 and T_d as in T_1, which indicated saturation of the sample number. Hence the threshold values were adjusted by referring to those critical values.

In the case of particles of 3·4 mm diameter, the size of particles was so large that the Doppler signals dropped out when the particles crossed the beam. It was therefore impossible to get any information about the 3·4 mm particles. On the other hand, the air-flow signals from small tracers were discriminated automatically from the frequency tracker output. Thus the comparator in the above signal-processing system was omitted in the experiment using 3·4 mm particles.

2.3. *Other remarks*

As is shown in figure 4, all the data were stoied in an analog data recorder (TEAC model R410). The data in the recorder were sampled at intervals of 0·025 ms and recorded on magnetic tape in digital form for subsequent numerical analysis by a large computer (FACOM M200). The records were over a period of 1·64 s (2^{16} readings).

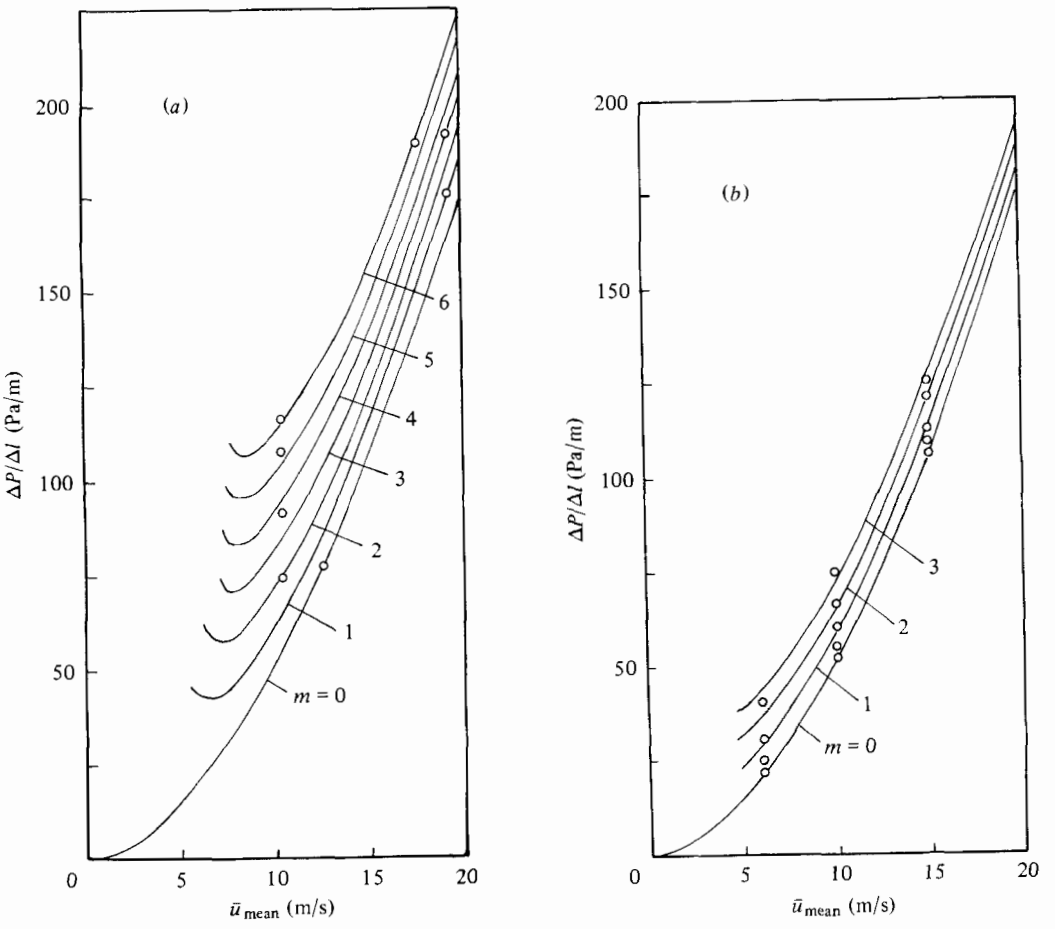

FIGURE 7. Relations between the pressure drop and superficial air velocity: (*a*) 3·4 mm particles; (*b*) 0·2 mm particles.

The mean air velocity was also measured using a Pitot tube, the results of which were compared with those of LDV.

The air–solid two-phase flow in the horizontal pipe generally has an asymmetric structure in the vertical direction, which is due to the effect of gravity. The gravitational force makes the flow more complicated in the horizontal pipe than in the vertical one, as was mentioned by Owen (1969). The weakness of the one-dimensional theory of the two-phase flow is caused by this asymmetric structure. Since we had an interest in the asymmetry, we traversed the measuring point (scattering volume) vertically in the horizontal pipe. Although the traversing itself could be done satisfactorily by an appropriate mechanism, the effect of refraction had to be taken into consideration because the angle between the beam and the pipe wall changed during traversing. Therefore deviation of the measuring point from an expected position due to the refraction was calculated, based on the geometrical optics. As a result, we confirmed that the influence of refraction could be neglected so long as the traversing was made in the range $|r| < 14$ mm in the case of the present pipe, 30·5 mm in diameter.

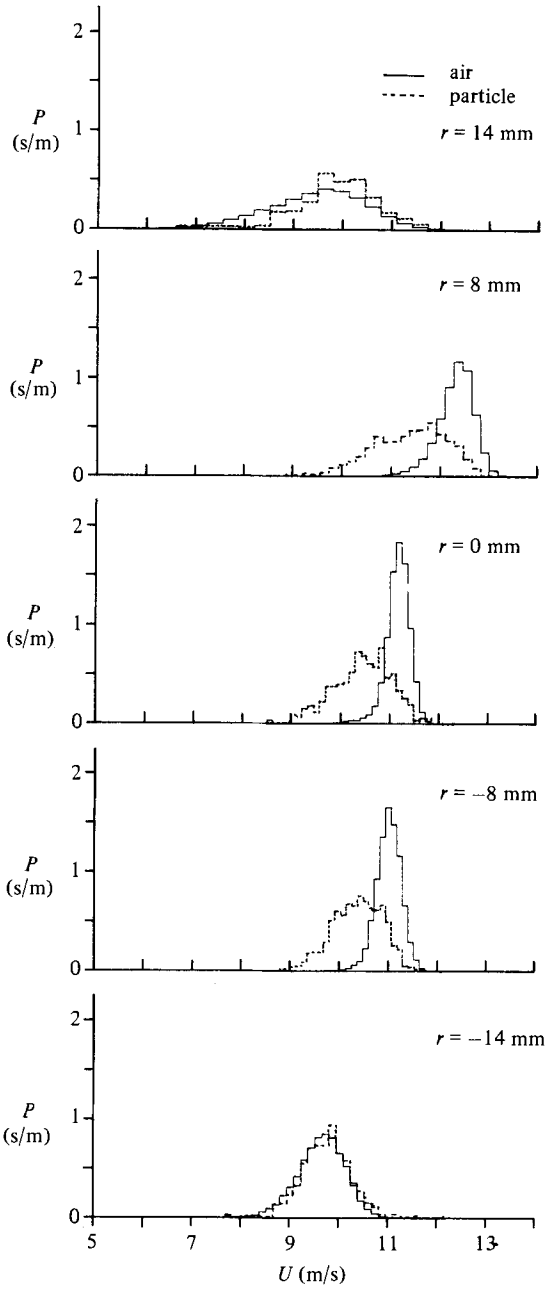

FIGURE 8. Probability densities of air and 0·2 mm particle velocities.

3. Results

3.1. *Pressure drop*

The relation between the pressure drop and the air velocity is the most important in designing pneumatic-conveying facilities. Although our main interests are in the basic aspects of the phenomena in the pipe, it is necessary to know where the present results

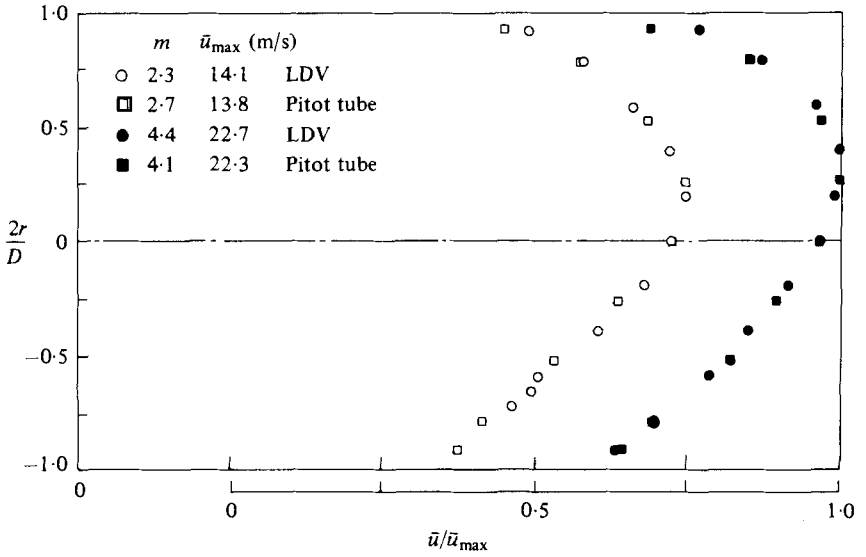

FIGURE 9. Comparison of mean air velocities by a Pitot tube and LDV in the presence of 3·4 mm particles.

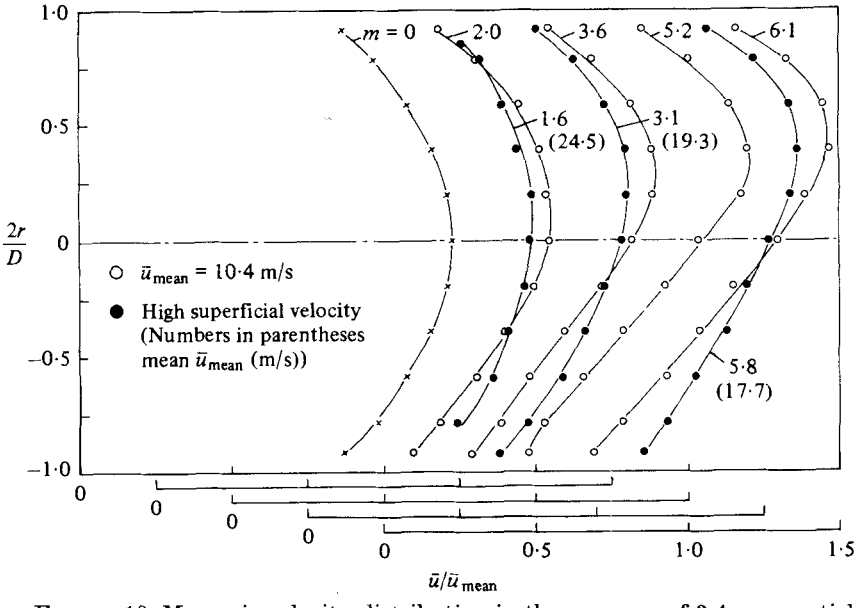

FIGURE 10. Mean air-velocity distribution in the presence of 3·4 mm particles.

are situated in the pressure-drop *vs.* air-velocity diagram. The diagrams are shown in figure 7, where $\Delta P/\Delta l$ is the pressure drop per unit pipe length at the measuring section, $\bar{u}_{mean}$ is the superficial air velocity, defined as the velocity averaged over the pipe cross-section, and m is the loading ratio, defined as the solids-to-air mass-flow rates ratio. Several curves are based on the experimental results, and plotted points correspond to the present LDV experiments. The loading ratios m or solid concentrations were adjusted to be small compared with the conditions in practical conveying, because measurements of the forward-scattered-light mode were difficult at a

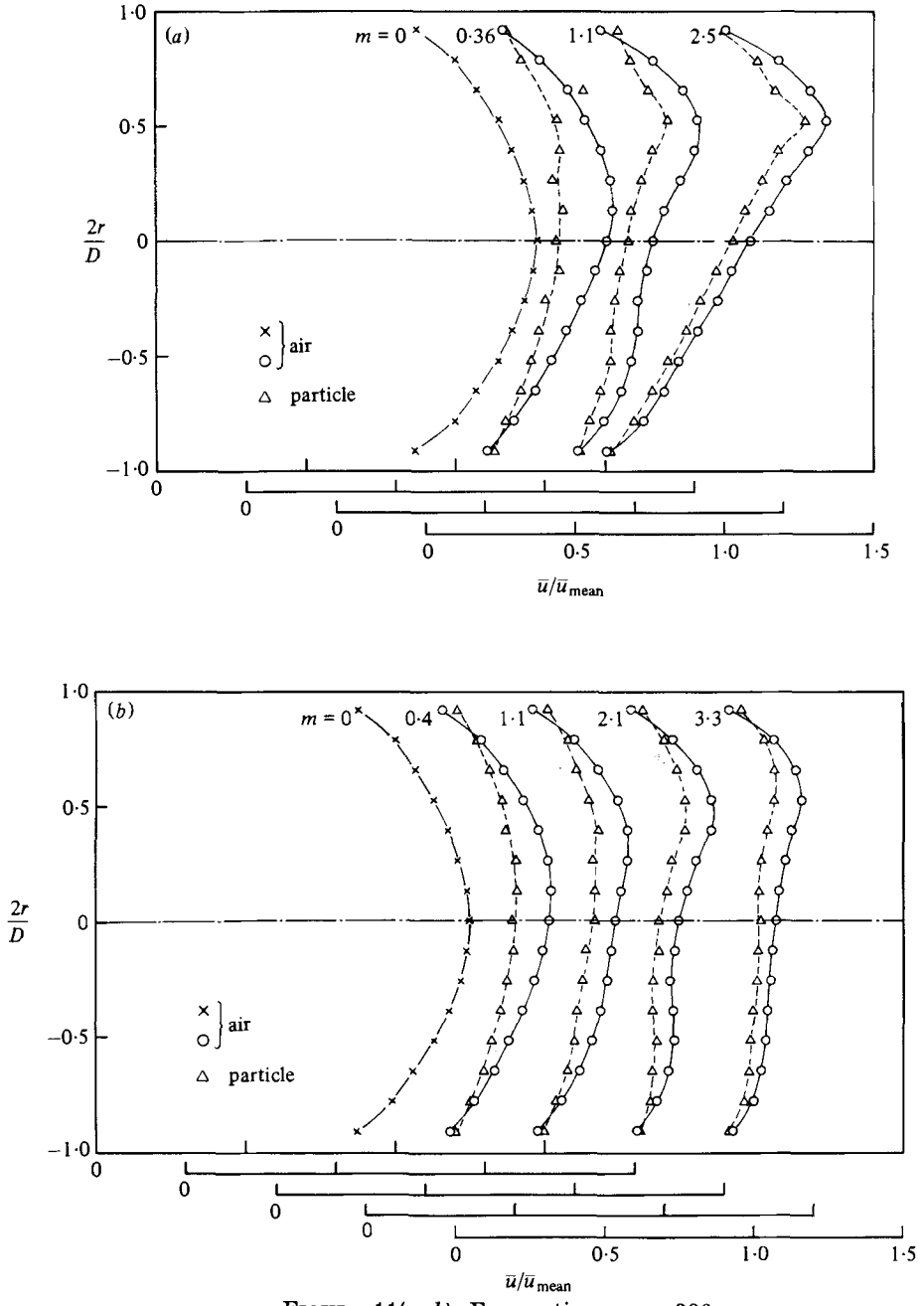

FIGURE 11(*a*, *b*). For caption see p. 396.

large loading. As is well-known, the total pressure drop in a dilute phase transportation is the sum of the pressure drop due to the air only and the additional drop due to the particles. The pressure drop due to the air is proportional to $\bar{u}^2_{\text{mean}}$ at a large Reynolds number, while the additional drop is inversely proportional to $\bar{u}^n_{\text{mean}}$, where n is determined empirically. Therefore the total pressure drop has a minimum value at a certain value of the velocity $\bar{u}_{\text{mean}}$.

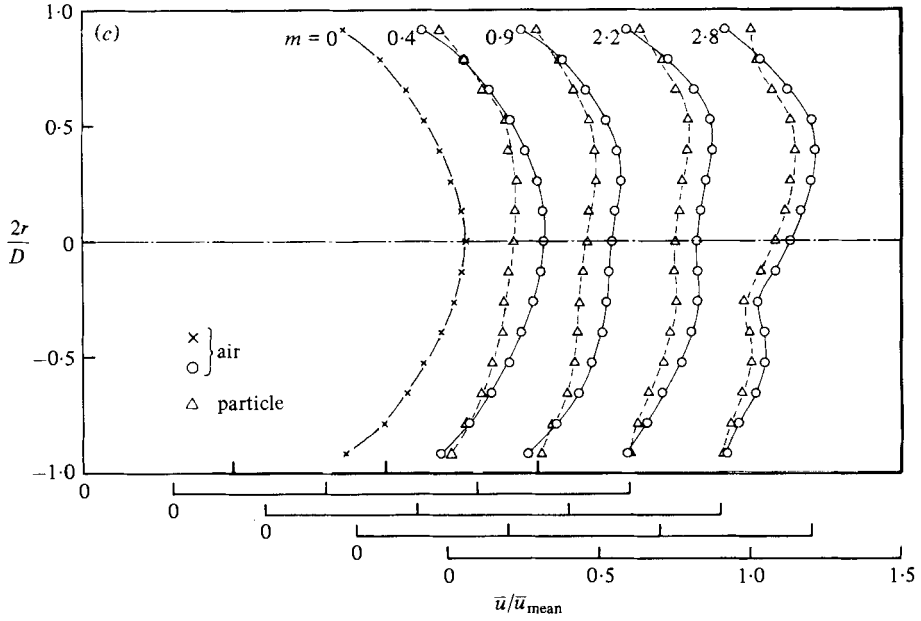

FIGURE 11. Mean velocity distributions of air and 0·2 mm particles: (*a*) $\bar{u}_{\text{mean}}$ = 6 m/s; (*b*) 10 m/s; (*c*) 15 m/s.

3.2. *Probability densities of air and particle velocities*

Whether signals are discriminated correctly between air and particles is checked by using the probability densities of both velocities. Figure 8 shows examples of probability densities. Generally, the velocity difference between air and particles is large near the pipe centre, and thus probability distributions at such a position deviate from each other. If the discrimination were incomplete, the probability density would show an unusual profile, because one of the signals would be taken partly for the other. Figure 8 does not show such an unusual shape, and therefore the signal discrimination is found to be satisfactory.

3.3. *Mean velocities of air and particles*

Figure 9 shows mean air velocities measured by LDV and a Pitot tube in the presence of 3·4 mm particles, where $\bar{u}_{\text{max}}$ is the maximum velocity in the section and r is the vertical distance measured from the pipe axis with the upward direction positive. The outer and inner diameters at the open end of the Pitot tube were 1 and 0·6 mm, respectively. The figure indicates that the results of both methods show good agreement, meaning that an ordinary Pitot-tube method is useful in the two-phase flow of coarse particles so far as the mean velocity of air phase is concerned.

Figure 10 shows mean air velocity profiles in the presence of 3·4 mm particles measured by LDV with different superficial air velocities and loading ratios. The profiles show asymmetric distributions, and the points corresponding to the maximum velocities shift upward, as the loading ratio increases and the air velocity decreases. Solid particles tend to be distributed near the bottom side in the horizontal pipe because of the gravity force. As a result, fluid motion is more retarded there by the particles.

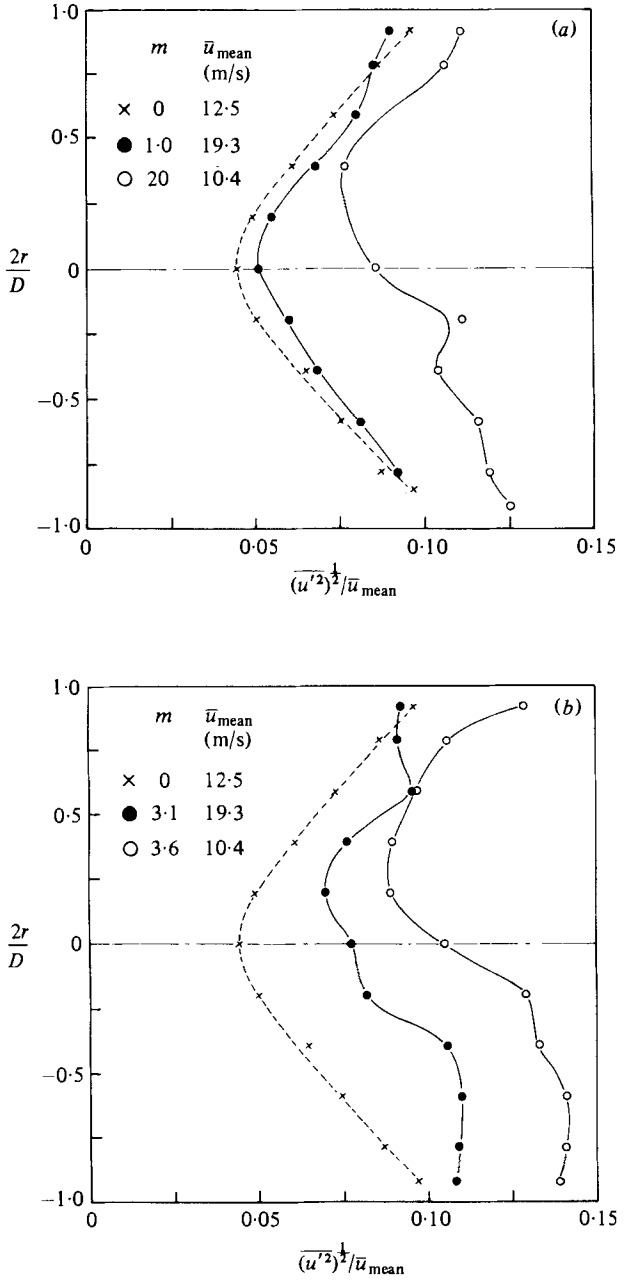

FIGURE 12(*a*, *b*). For caption see p. 398.

The same results have been already found by several workers using the Pitot tube (Welschof 1962).

Air and particle mean velocities in the presence of 0·2 mm particles are shown in figure 11. The figure shows a flattening of the particle-velocity profile compared with the air-velocity profile. As the case of 3·4 mm particles, asymmetric profiles are noticeable at low superficial air velocities and high loading ratios. When a comparison

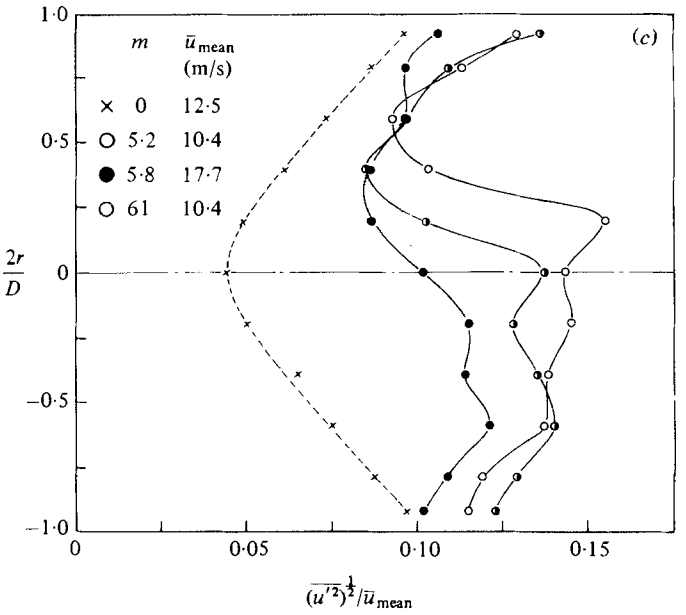

FIGURE 12. Turbulence intensity of air in the presence of 3·4 mm particles: (*a*) low loading ratio; (*b*) middle loading ratio; (*c*) high loading ratio.

is made between 0·2 mm particles and 3·4 mm ones at the same superficial air velocity, it is found that the flattening of the air-velocity profile is more remarkable in the case of 0·2 mm particles.

3.4. *Intensities of fluctuating velocities*

So far there have been very few measurements of the fluid turbulence in the air–solid two-phase flow in a pipe. Similar measurements of LDV to the present were made in a liquid–air two-phase flow in a vertical channel by Ohba & Yuhara (1979), and in a liquid–solid flow in a horizontal pipe by Zisselmar & Molerus (1979). However, the flow characteristics in those works are different from the present experiment in many respects. Some workers attempted to measure air turbulence in the air–solid two-phase flow before LDV was available. For example, Maeda, Mitsueda & Ikai (1976) and Maeda, Hishida & Furutani (1980) used a hot-wire anemometer in a flat-plate boundary layer and in a vertical pipe flow, and Soo, Ihrig & El Kouh (1960) used a tracer-diffusion technique in a square duct with helium as the tracer. In those works, measurements were restricted to the case of very low loading ratios or concentrations, and thus the effect of particles on the flow was not so marked. Figure 12 shows distributions of turbulence intensities $(\overline{u'^2})^{\frac{1}{2}}/\bar{u}_{\text{mean}}$ of air flow in the presence of 3·4 mm particles, where u' is the axial fluctuating component of air velocity. The figure indicates a large increase in the turbulence intensity caused by the particles. As the loading ratio increases, the turbulence increases from the bottom side, and shows an asymmetric distribution. This tendency becomes more noticeable at low superficial air velocities and high loading ratios, as in the case of the mean-velocity distribution. However, the turbulence intensity near the upper wall of the pipe does not increase very much. This is because the local concentration of the particles is low near the upper wall even at the high loading. Turbulence in the present test section was fully developed in the single

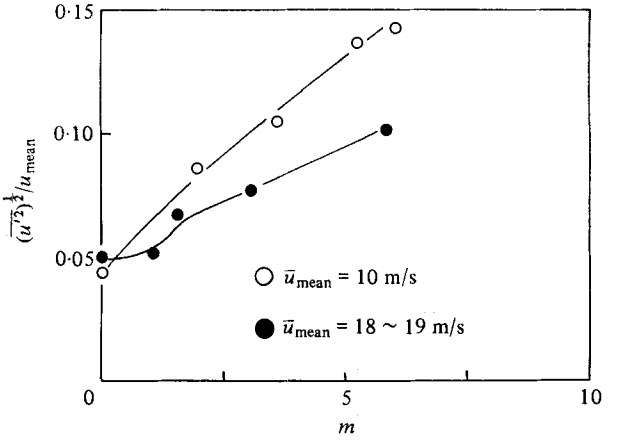

FIGURE 13. Relation between the turbulence intensity of air and loading ratio in the presence of 3·4 mm particles (pipe axis).

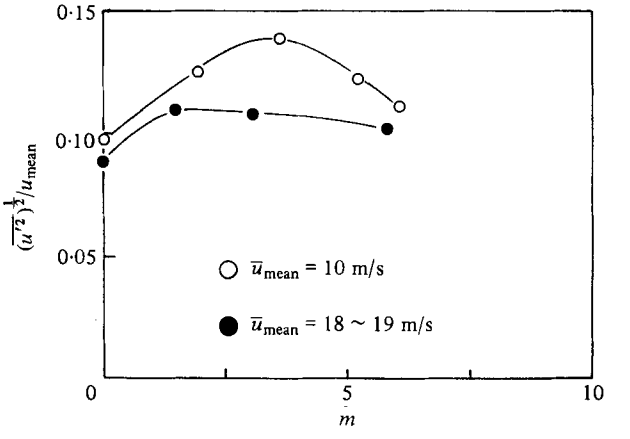

FIGURE 14. Relation between the turbulence intensity of air and loading ratio in the presence of 3·4 mm particles ($2r/D = -0{\cdot}918$).

phase, and therefore the increase in turbulence due to the particles means that the turbulence produced by the particles overcomes that of the fully developed pipe flow. In other words, the turbulence is not suppressed by the particles, which is different from the case of fine particles shown later. In the case of coarse particles like 3·4 mm particles, the velocity difference between particles and air is usually large and each particle sheds a wake disturbance to the flow like a turbulence-generating grid. In order to confirm the mechanism of turbulence increase mentioned above, the Reynolds number of the flow around the particle is briefly discussed. The velocity ratio of particle to air can be estimated to be about 0·8 in the case of large particles like the 3·4 mm particle. Thus for, example, the velocity difference or relative velocity is 2 m/s when the mean air velocity is 10 m/s. The Reynolds number based on the relative velocity and particle diameter is about 470. At this Reynolds number, the particle sheds vortices vigorously, as many experiments have shown (Achenbach 1974).

Figure 13 shows the relation between the turbulence intensity at the pipe axis and the loading ratio. The intensity is proportional to the loading ratio within the range

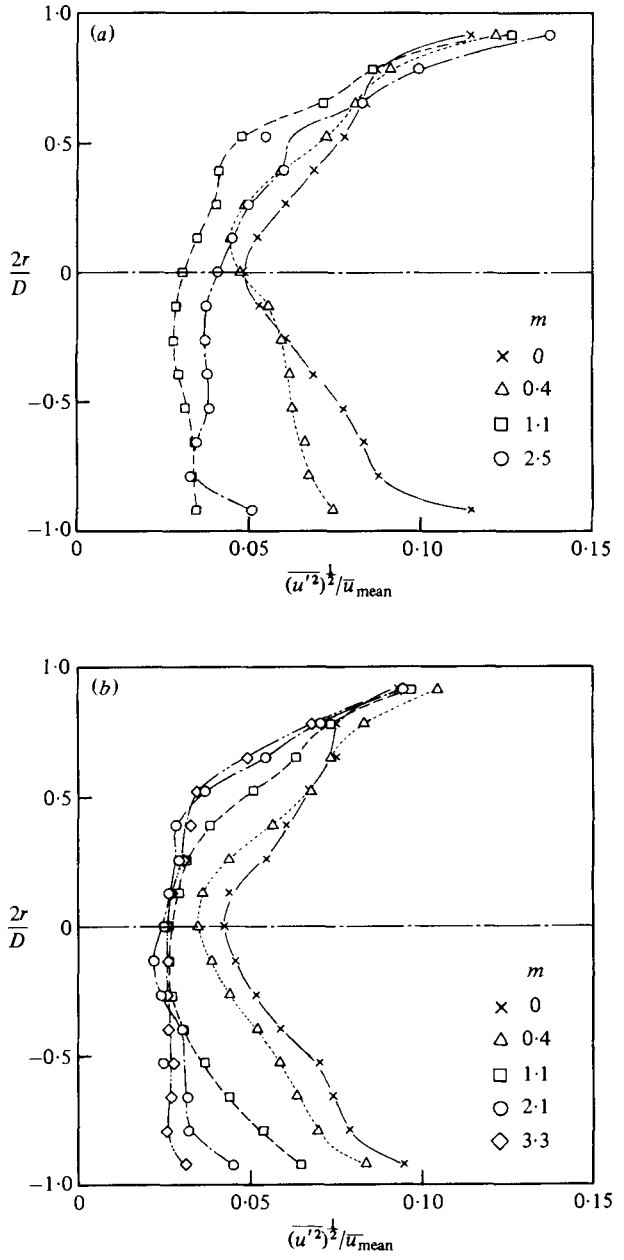

FIGURE 15(*a*, *b*). For caption see facing page.

of the present experiment. Figure 14 shows the turbulence intensity at $2r/D = -0{\cdot}918$. Some sign of turbulence suppression is observed near the bottom, although the particles increase the turbulence in most parts of the pipe section. That is, the turbulence intensity begins to decrease near the bottom as the loading ratio exceeds a certain value. Generally, the pipe flow has the maximum intensity near the wall. Near the bottom wall, the velocity difference between both phases is small and the particle concentration is high. In such a place, the particles tend to act as a damper

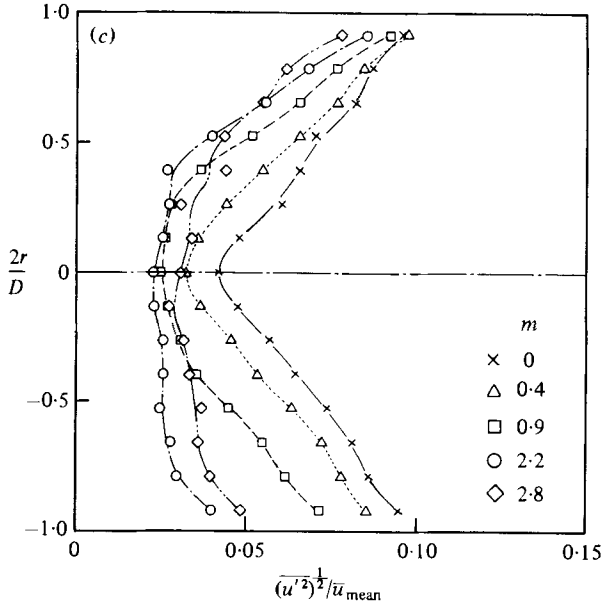

FIGURE 15. Turbulence intensity of air in the presence of 0·2 mm particles. (*a*) $\bar{u}_{\text{mean}}$ = 6 m/s; (*b*) 10 m/s; (*c*) 15 m/s.

against the existing turbulence. Figures 13 and 14 show that the intensity is smaller at a lower air velocity. That may be because the particle free path is shorter at a low velocity, and thus the particles cross the mean flow more frequently than at a high velocity.

Figure 15 shows the turbulence intensity of air flow in the presence of 0·2 mm particles. It is found that the turbulence is greatly suppressed, in contrast to the case of 3·4 mm particles. Reduction in the intensity is more remarkable in the lower half of the pipe section, which is due to the high concentration of the particles. The turbulence intensity decreases with increasing loading ratio. As the loading ratio becomes larger, the region of low turbulence intensity spreads over the section, but the minimum level of the intensity remains the same. In the present stage, we cannot decide whether the reduction is really saturated, because the accuracy of LDV is not good enough in the case of small turbulence. Nevertheless we can conclude from a comparison between the results of 3·4 and 0·2 mm particles that the effects of the particles on the air turbulence are very different with the particle size. As is pointed out, the accuracy of LDV measurement of turbulence is worse than the hot-wire anemometer. However, the change in turbulence due to the particle is so remarkable that what is mentioned above is not affected by the measuring error, at least qualitatively.

The foregoing results raise a problem in the theoretical treatment of the two-phase flow in the pipe. Most previous theories dealing with particle motion have made use of the drag force on the particle, which was obtained in a uniform laminar flow. As was shown by Torovin & Gauvin (1960), the drag force is largely affected by the free-stream turbulence, and thus the turbulence should be taken into account in the calculation of particle motion. In addition to that, the present results imply that information about

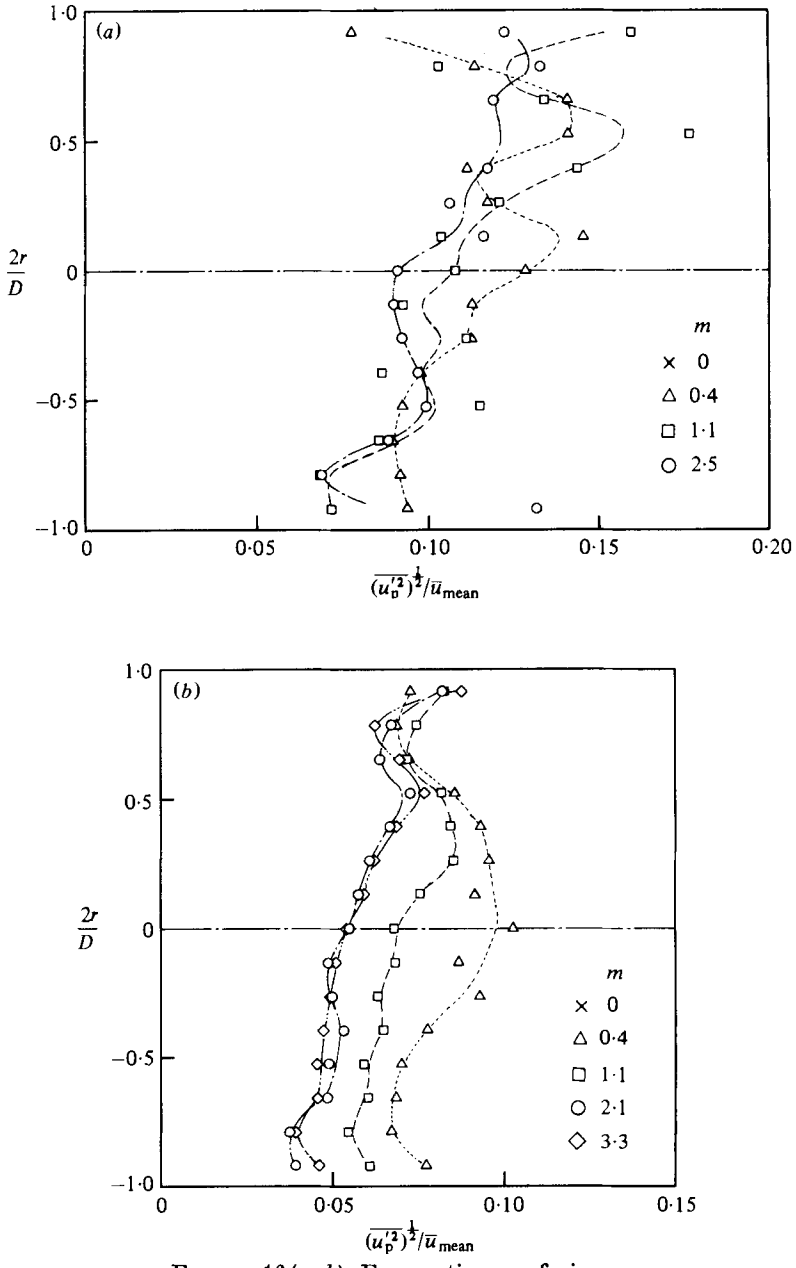

FIGURE 16 (*a*, *b*). For caption see facing page.

turbulence in a single phase pipe flow is not accurate in the two-phase flow, because the existing turbulence is also affected by the presence of particles.

Figure 16 shows the intensity of fluctuating velocity of 0·2 mm particles (standard deviation). The fluctuation decreases as the loading ratio increases. The distribution of the fluctuation is generally flat and uniform, although it shows a maximum value near the pipe centre at a low loading ratio. The intensity is a little higher in the upper half of the section. Comparatively fine particles like 0·2 mm particles follow the mean

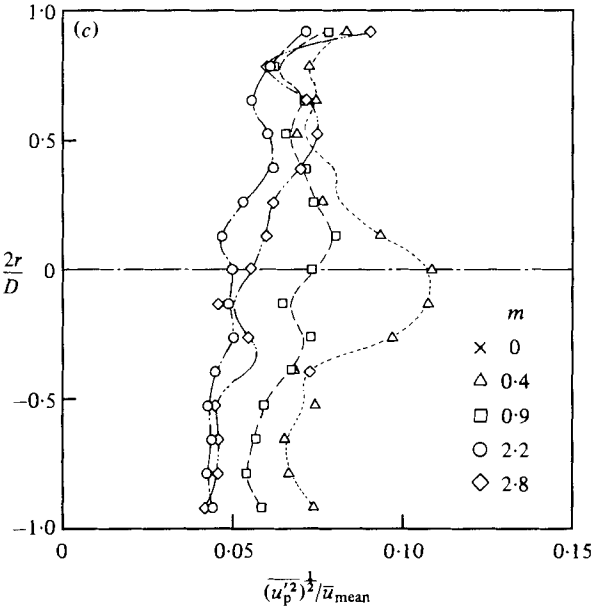

FIGURE 16. Intensity of fluctuating velocity of 0·2 mm particles: (*a*) $\bar{u}_{mean}$ = 6 m/s; (*b*) 10 m/s; (*c*) 15 m/s.

air velocity to some extent, but not the air turbulence. Small tracers for the air-flow measurement can be assumed approximately to form a continuous medium at a high concentration, but particles larger than several hundreds of micrometres cannot be regarded as such a continuous phase, even as an approximation. Therefore the velocity fluctuation of those particles has a different mechanism from the air-flow turbulence. Namely, the difference in the particle size and the collision of particles are the causes of fluctuation.

3.5. *Skewness and flatness*

In §3.2 we showed the probability-density functions of air and particle velocities to check the signal discrimination. It is meaningful to compare the single- and two-phase flows in the probability-density function of air flow when one is interested in characteristics of air turbulence in the presence of particles. The properties of the probability density curve can be expressed in terms of the skewness and flatness factors

$$S = \overline{u'^3}/(\overline{u'^2})^{\frac{3}{2}},$$

$$F = \overline{u'^4}/(\overline{u'^2})^2.$$

Figures 17 and 18 show the distributions of these factors. When the probability follows the Gaussian distribution, S and F take the values 0 and 3 respectively. The figures indicate that the probability in the two-phase flow deviates from the Gaussian, i.e. it has flatness larger than 3 and negative skewness. The reason for the above results is as follows. Large particles have generally smaller velocities than the mean air velocity, and they are thus accompanied by wakes. The moment that such a particle passes at or around the measuring point, the instantaneous air velocity takes a small and peaked

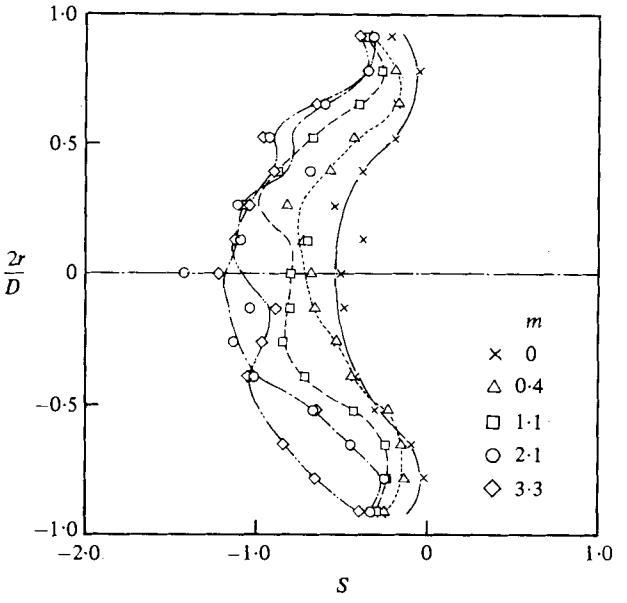

FIGURE 17. Skewness factor of air turbulence in the presence of 0·2 mm particles ($\bar{u}_{\text{mean}}$ = 10 m/s).

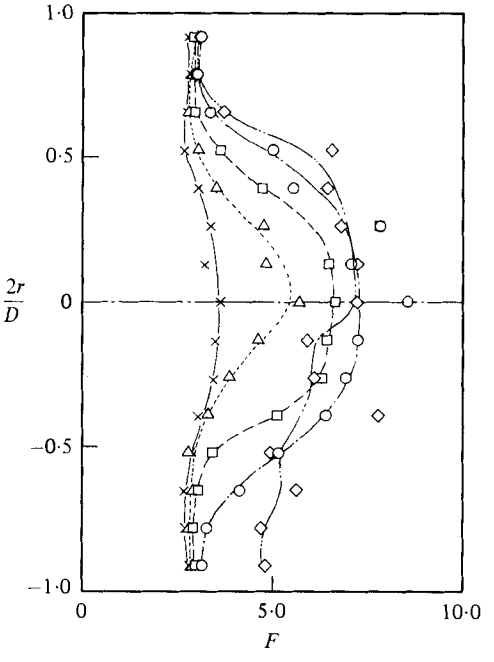

FIGURE 18. Flatness factor of air turbulence in the presence of 0·2 mm particles ($\bar{u}_{\text{mean}}$ = 10 m/s).

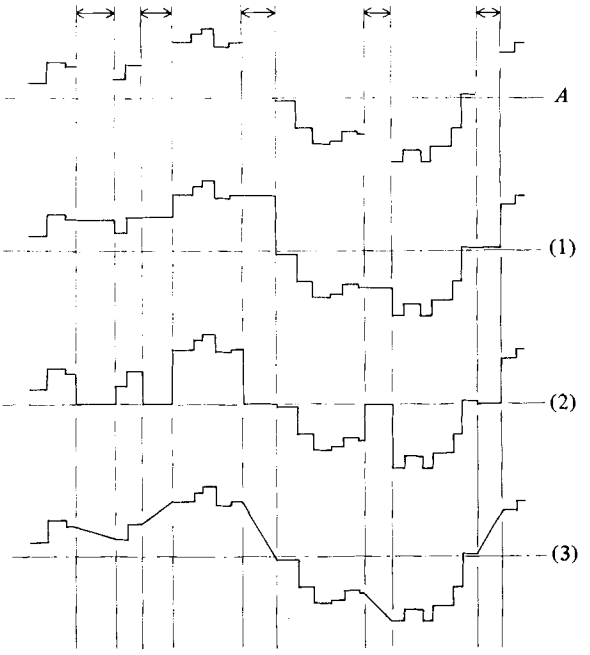

FIGURE 19. Simulation signals and interpolation scheme for defective parts: ↔, defective part.

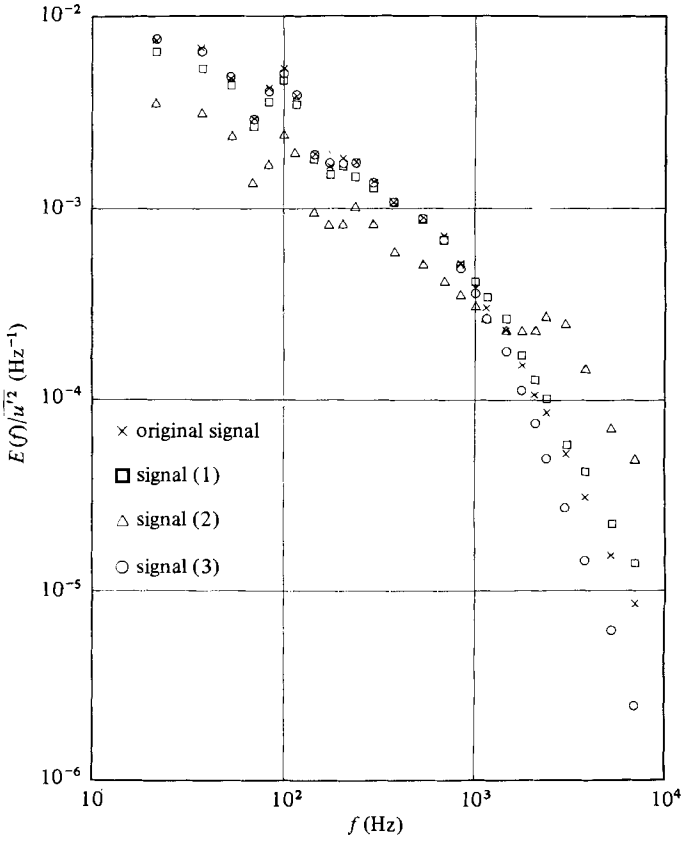

FIGURE 20. Frequency power spectrum of the simulation signal.

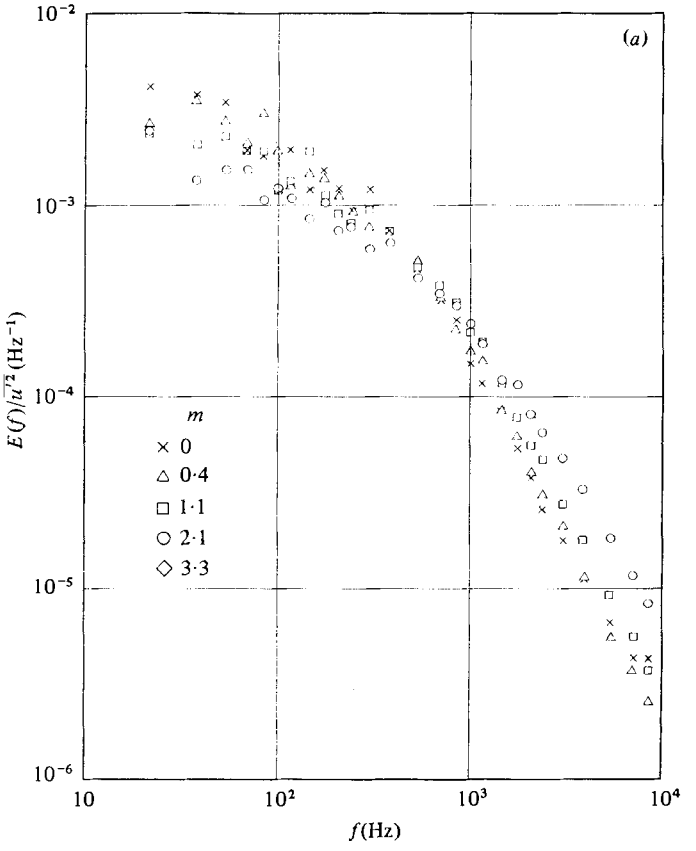

FIGURE 21 (*a*). For caption see p. 408.

value owing to the effect of the wake. As a result, the probability function becomes asymmetric, having a long skirt on the side of low velocity and showing negative skewness and large flatness. Near the pipe wall, the velocity difference is generally small, and thus the effect of the particles on the probability function is weak.

3.6. *Frequency spectrum of air turbulence*

It is not an easy task to obtain frequency power spectra of turbulence in air–solid two-phase flows. As long as LDV is used, the calculated spectrum is limited to a not-too-high frequency range, because the signal from the tracker is more or less discontinuous. Even when the concentration of tracers is high enough to detect small-scale turbulence, it is difficult to obtain the spectra at high frequency, because the tracers cannot follow the motion at high frequency, and because LDV has inherent noise problems in the high-frequency range, as is mentioned by several workers (George 1975). Besides the above difficulties, there is another problem in the two-phase flow. The time-sequence signal is interrupted by the presence of large particles. The parts of signals corresponding to the large particles or the parts that are determined to be ambiguous in the discrimination circuit are missing for the air signal. The spectrum of the signal having such intermittent defects can be obtained by the Fourier transformation of the autocorrelation function which is calculated by excluding the defective

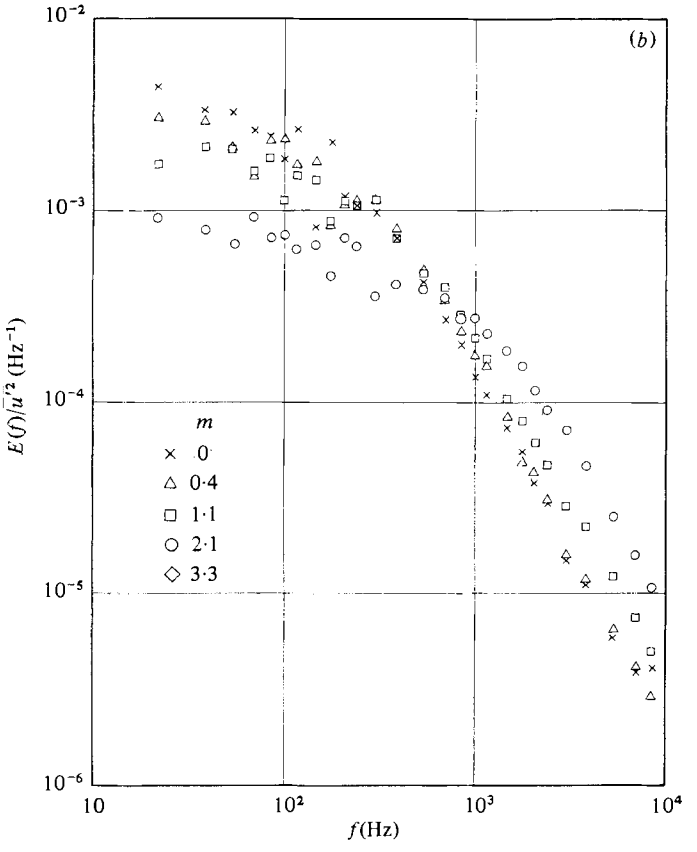

FIGURE 21 (*b*). For caption see p. 408.

parts. However, this method requires much computer time. Hence we attempted to calculate the spectra by the use of the fast Fourier transform (FFT), in which the defective parts are interpolated by suitable lines. In the case of 0·2 mm particles, the time length of one defect is so short that the spectrum calculation can be done satisfactorily if proper interpolation lines are chosen. In order to find the proper line, we made the following preliminary calculation. A waveform of single-phase air flow was taken and recorded on magnetic tape in digital form. First the spectrum of this wave was obtained by FFT. Then a number of defects were given to the above wave artificially, and a simulation signal similar to the two-phase flow was produced like signal *A* in figure 19. Intervals and lengths of the defect occurrences in the simulation signal were given by referring to the real two-phase-flow signal and using random numbers. Since the spectrum with no defect is known and regarded as the true spectrum, various interpolation schemes can be assessed by comparing the resulting spectrum with the true one. The following three interpolation lines are attempted. The first one is to hold the value before the defect, the second is to replace the defective part by the average value which is zero for the alternating component, and the third is to replace the defective part by a straight line connecting normal parts. The above interpolations are discussed in the paper by Buchhave, George & Lumley (1979), who introduced them to cope with the signal dropout due to scanty tracers. Figure 20 shows a comparison in spectra between the three methods. The desirable interpolation is that which

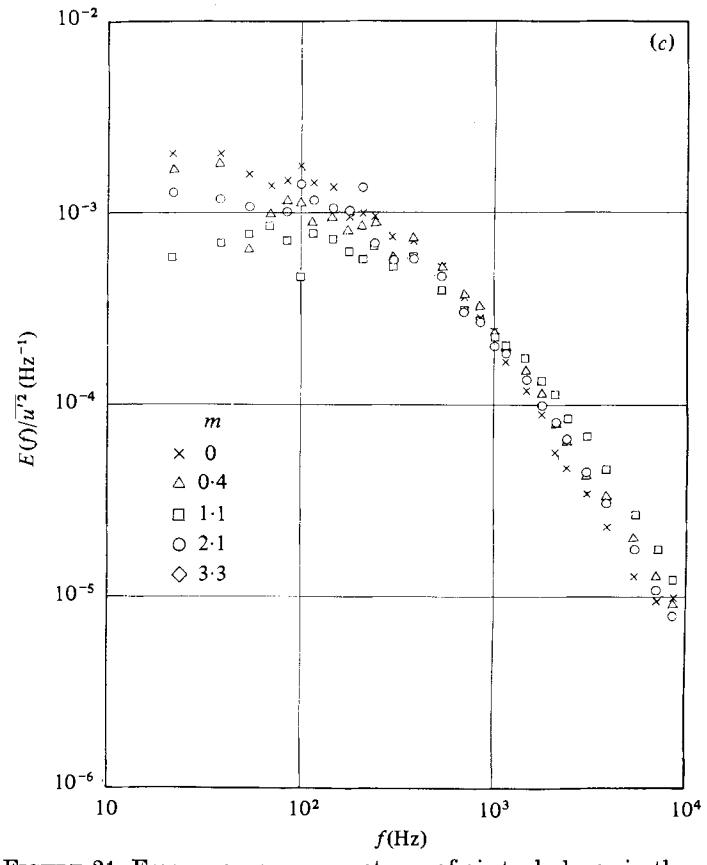

FIGURE 21. Frequency power spectrum of air turbulence in the presence of 0·2 mm particles ($\bar{u}_{\text{mean}}$ = 10 m/s): (*a*) r = 8 mm; (*b*) 0 mm; (*c*) −8 mm.

gives good agreement with the spectrum of the signal with no defect marked (×) in the figure. It is found in the figure that the first method is among the best, although it exaggerates the high-frequency component a little. The result of the second differs largely from the true spectrum. The third method estimates the high-frequency part less accurately, but we adopted this method to calculate the spectra of the two-phase air flow; the reason for this is mentioned below. While figure 20 shows the results near the bottom wall of the pipe, the same tendency was observed at other parts of the pipe section.

Figure 21 shows the frequency power spectra of air turbulence in the presence of 0·2 mm particles, where the spectra are normalized by $\overline{u'^2}$. The figure indicates that the spectral components at high-frequency increase with increasing loading ratio. As was mentioned above, to calculate the spectrum we used the third interpolation method which tends to underestimate high-frequency parts. In spite of this tendency, the high-frequency parts increase in the presence of particles. The reason we adopted the third interpolation method is to obtain the present results more confidently.

The authors are very grateful to Mr S. Takahashi and Mr T. Uwaji who carried out the experiment with great competence and enthusiasm. This work was partially supported by the Grant-in-Aid for Scientific Research from the Ministry of Education in Japan.

REFERENCES

ACHENBACH, E. 1974 Vortex shedding from spheres. *J. Fluid Mech.* **62**, 206.

ADAM, O. 1957 Feststoffbeladene Luftströmung hoher Geschwindigkeit. *Chem. Ing. Tech.* **29**, 151.

BIRCHENOUGH, A. & MASON, J. S. 1976 Local particle velocity measurements with a laser anemometer in an upward flowing gas–solid suspension. *Powder Tech.* **14**, 139.

BUCHHAVE, P., GEORGE, W. K. & LUMLEY, J. L. 1979 The measurement of turbulence with the laser-Doppler anemometer. *Ann. Rev. Fluid Mech.* **11**, 443.

DOIG, I. D. & ROPER, G. H. 1967 Air velocity profiles in presence of concurrently transported particles. *Ind. & Engng Chem. Fund.* **6**, 247.

DURST, F., MELLING, A. & WHITELAW, J. H. 1976 *Principles and Practice of Laser-Doppler Anemometry*, p. 303. Academic.

DURST, F. & UMHAUER, H. 1975 Local measurements of particle velocity, size distribution and concentration with a combined laser Doppler particle sizing system. In *Proc. LDA Symp., Copenhagen*, p. 430.

GASTERSTÄDT, J. 1924 Die experimentelle Untersuchung des pneumatischen Fördervorganges. *Forsch. Arb. Ing. Wes.* no. 265.

GEORGE, W. K. 1975 Limitations to measuring accuracy inherent in the laser Doppler signal. In *Proc. LDA Symp., Copenhagen*, p. 20.

JOTAKI, T. & TOMITA, Y. 1971 Solids velocities and pressure drops in a horizontal pneumatic conveying systems. In *Proc. 1st Conf. Pneumatic Transport of Solids in Pipes, BHRA Fluid Engng*, paper B3.

KRAMER, T. J. & DEPEW, C. A. 1972 Experimentally determined mean flow characteristics of gas–solid suspensions. *Trans. A.S.M.E.* D, *J. Fluids Engng* **94**, 492.

MAEDA, M., MITSUEDA, T. & IKAI, S. 1976 The investigation of heat transfer in a gas–solid two phase flow (the 1st report, experiment and discussion of the heat transfer by the free stream turbulence) (in Japanese). *Trans. Japan Soc. Mech. Engrs*, series 2, **42**, 866.

MAEDA, M., HISHIDA, K. & FURUTANI, T. 1980 Velocity distributions of air–solid suspension in upward pipe flow (effect of particles on air velocity distribution) (in Japanese). *Trans. Japan Soc. Mech. Engrs* B **46**, 2313.

OHBA, K. & YUHARA, T. 1979 Velocity measurements of both phases in two-phase flow using laser doppler velocimeter. In *Proc. IMEKO Symp., Tokyo*, p. 181.

OWEN, P. R. 1969 Pneumatic transport. *J. Fluid Mech.* **39**, 407.

SOO, S. L., IHRIG, H. K. & EL KOUH, A. F. 1960 Experimental determination of statistical properties of two-phase turbulent motion. *Trans. A.S.M.E.* D, *J. Fluids Engng* **82**, 609.

TOROVIN, L. B. & GAUVIN, W. H. 1960 Fundamental aspects of solids–gas flow. Part 5. The effects of fluid turbulence on the particle drag coefficient. *Can. J. Chem. Engng* **38**, 189.

WELSCHOF, G. 1962 Pneumatische Förderung bei grossen Fördergutkonzentrationen. *VDI Forsch.* no. 492.

ZISSELMAR, R. & MOLERUS, O. 1979 Experimentelle Untersuchungen zum Turbulenzverhalten der Suspensionsströmung in horizontalen Rohrleitungen. *Chem. Ing. Tech.* **51**, 50.